Neurocomputing xxx (xxxx) xxx

Contents lists available at ScienceDirect

Neurocomputing

journal homepage: www.elsevier.com/locate/neucom

Computer aided Alzheimer's disease diagnosis by an unsupervised deep learning technology

Xiuli Bi[a], Shutong Li[a], Bin Xiao[a,*], Yu Li[b], Guoyin Wang[a], Xu Ma[c]

[a] Chongqing Key Laboratory of Computational Intelligence, Chongqing University of Posts and Telecommunications, Chongqing 400065, China
[b] School of Information Technology and Electrical Engineering, The University of Queensland, Brisbane 4072, Australia
[c] Human Genetics Resource Center, National Research Institute for Family Planning, Beijing 100081, China

ARTICLE INFO

Article history:
Received 31 May 2018
Revised 26 October 2018
Accepted 12 November 2018
Available online xxx

Keywords:
Deep learning
Unsupervised learning
Convolutional neural network
Alzheimer's disease prediction
Magnetic Resonance Imaging data
Computer aided diagnosis

ABSTRACT

Deep learning technologies have played more and more important roles in Computer Aided Diagnosis (CAD) in medicine. In this paper, we tackled the problem of automatic prediction of Alzheimer's Disease (AD) based on Magnetic Resonance Imaging (MRI) images, and propose a fully unsupervised deep learning technology for AD diagnosis. We first implement the unsupervised Convolutional Neural Networks (CNNs) for feature extraction, and then utilize the unsupervised predictor to achieve the final diagnosis. In the proposed method, two kinds of data forms, one slice and three orthogonal panels (TOP) of MRI image, are employed as the input data respectively. Experimental results run on all the 1075 subjects in database of the Alzheimer's Disease Neuroimaging Initiative (ADNI 1 1.5T) show that the proposed method with one slice data yields the promising prediction results for AD vs. MCI (accuracy 95.52%) and MCI vs. NC (accuracy 90.63%), and the proposed methods with TOP data yields the best overall prediction results for AD vs. MCI (accuracy 97.01%) and MCI vs. NC (accuracy 92.6%).

1. Introduction

Alzheimer's Disease (AD) is a progressive brain disorder and the most common of dementia in the late life. AD leads to the death of nerve cell and tissue loss throughout the brain, thus reducing the brain volume in size dramatically through time and affecting most of its function [1]. The estimated number of affected people will double for next two decades, so that one out of 85 persons will have the AD by 2050 [3]. Because the cost of caring the AD patients is expected to rise dramatically, the necessity of having a computer aided diagnosis (CAD) system for early and accurate AD diagnosis becomes critical [4]. Moreover, Mild Cognitive Impairment (MCI) is an intermediate stage between Normal Cognition (NC) and clinical dementia. Exiting study [6] has shown that MCI subjects progress to clinical AD with an annual rate of approximately 10–15%. Research on identifying MCI individuals who will progress to clinical dementia has received increasing attention in recent years [7].

Among many modalities of medical images, Magnetic Resonance Imaging (MRI), Computed Tomography (CT), and Positron Emission Tomography (PET) scans contain information about the effects of AD on the structure and function aspects. Compared with MRI, CT and PET, MRI is the most standardized and widely available imaging modality in clinical practice [8], and MRI examinations can provide an opportunity to track different clinical phases of AD. However, analyzing such MRI images consumes more time for doctors and researches because each image contains millions of voxels and tremendous information.

There are many functional connectivity modeling methods proposed for AD diagnosis, including the correlation-based methods [9], graphical models [10] partial-correlation-based methods [11], and sparse representation-based methods [12]. Furthermore, several types of features [12,13,21,23,26] were extracted from MRI image for AD prediction, such as gray matter density maps, cortical thickness as well as volume and shape measures. Another popular method [7] achieves the classification through segmenting the whole brain into multiple anatomical or discriminative regions and then extracting regional features. Some recent methods [14] introduced that the features extracted from neuroimaging data are not isolated and exhibit high correlations. Considering the relationships among these features, tree guided sparse coding methods [16] and re-sampling schemes using Elastic net [17] have been proposed for AD diagnosis. Although the low-level features can be hand crafted with great success for certain applications, most of the hand-crafted features cannot be adapted to new condition because designing effective features for new situations usually requires new domain knowledge. Learning features from data of interest is considered as a plausible method of remedying the limitations of hand-crafted features.

* Corresponding author.
E-mail address: xiaobin@cqupt.edu.cn (B. Xiao).

https://doi.org/10.1016/j.neucom.2018.11.111
0925-2312/

Deep learning systems are more effective in many research areas, such as image object detection [2], image segmentation [5], image saliency detection [9], image classification [15] and remote sensing image processing [19]. These systems have the ability to extract high-level features from raw sensory data after using statistical learning over a large amount of data to obtain an effective representation of input data space. Among those systems, the convolutional neural network (CNN) is a popular form since it achieved breakthrough performance in AD diagnosis. Hosseiniasl et al. [18] presented the deep 3D-CNN for learning generic and transferable features across different domains, and it can detect the characteristic AD biomarkers in one (source) domain and perform task specific classification in another (target) domain. Choi and Jin [20] developed a deep CNN-based method for prediction of cognitive decline and selection of subjects who would eventually convert to AD. Sarraf et al. [22] outlined the deep learning-based pipelines which was employed to distinguish Alzheimer's MRI and fMRI from normal healthy control data for a given age group. Hosseini-Asl et al. [23] proposed a method to predict the AD with a deep 3D convolutional neural network, which is pre-trained to capture anatomical shape variations in structural brain MRI scans. Liu et al. [24] constructed a cascaded CNNs structure to learn the multi-level and multimodal features of MRI and PET brain images for AD diagnosis. Farooq et al. [25] proposed a CNN-based pipeline for the diagnosis of Alzheimer's disease and its stages using MRI images.

Although CNN-based methods could learn highly discriminative feature in medical images, there often arises the issue that labeled data is often not enough to learn the filter banks in CNNs, especially in medical applications. CNNs are unable to train in parameter setting and learn highly discrimination visual features when insufficient labeled datasets for training are available. This is the reason that few studies have been investigated in applying CNN to medical analysis due to the rare availability of labeled medical image data. Recently, an investigation [27] showed that the unsupervised CNN learns the filter banks by a traditional unsupervised machine learning algorithm can extract the features successfully in image classification tasks. This investigation employed the unsupervised CNN structure to learn the features and followed by a support vector machine (SVM) classifier to achieve the final classification result. However, the SVM is a supervised machine learning method which still requires labeled data to train and test the classifier. Therefore, how to develop a fully unsupervised method for achieving the medical image classification is still an open problem.

The fully unsupervised deep learning framework for medical image classification, in our opinion, mainly contains two parts. The first part is how to learn the features from input data by some unsupervised machine learning methods. And the second part is how to utilize the unsupervised classification methods to achieve the final classification results. In this paper, we focus on the problem of insufficient labeled data available in medicine, and propose a fully unsupervised deep learning technology for AD diagnosis. The proposed method includes the following two parts. Firstly, we employ an unsupervised CNN named PCANet for achieving the feature learning on MRI images. PCANet can learn the filters in CNNs by a traditional unsupervised machine learning algorithm and extract the features through the first convolution stage, the second convolution stage and the output stage. The main superiority of PCANet is that it doesn't involve the stochastic gradient descent (SGD) method that requires a large number of labeled data, and critically depends on expertise in parameter tuning and various ad hoc tricks. Secondly, we address the unsupervised classification method that is based on k-means to achieve the final prediction for AD diagnosis. Moreover, two different views of MRI image are introduced as input data in the proposed method, which includes one view of MRI image and three orthogonal panels (TOP) data from the three orthogonal views.

The remainder of this paper is organized as follows. Section 2 provides a brief introduction on PCANet and k-means. The proposed method for AD prediction are presented in details in Section 3. Section 4 describes the experiments and comparative analysis. A discussion is provided in Section 4. Section 5 concludes this paper.

2. Preliminaries

In this section, we provide the detailed descriptions on PCANet and k-means as preliminaries, and they will be utilized throughout the proposed work in this paper.

2.1. PCANet

The PCANet [27] employs two stages convolution filters learned by principal component analysis for feature mapping, and binary block-wise histograms for outputting features. Specifically, PCANet firstly unsupervised learn the abstract feature of object by exploiting classic PCA algorithms with recent deep learning representation architectures. The eigenvectors which corresponding to larger eigenvalues are treated as the learned filter banks in the first two convolution layers. This is followed by simple binary hashing and block histograms for indexing and pooling the features. The main steps of PCANet mainly includes the first convolution stage, the second convolution stage, and the output stage (including Hashing and Histogram generating).

2.1.1. The first convolution stage

Given N input training MRI images of size $r \times s$, for the i-th image $I_i \in \mathbb{R}^{r\times s}$, $i \in [1, N]$, we take a patch of size $k_1 \times k_2$ around each pixel, collect all the overlapping patches, vectorize them and combine them into a matrix $\mathbf{X}_i$ of $k_1 \times k_2$ rows and $(r - k_1 + 1) \times (s - k_2 + 1)$ columns. We then subtract patch mean from each patch for all the input images and combining them to obtain

$$\mathbf{X}=\left[\bar{\mathbf{X}}_1,\bar{\mathbf{X}}_2,\ldots,\bar{\mathbf{X}}_N\right] \in \mathbb{R}^{k_1k_2\times N(r-k_1+1)(s-k_2+1)}. \quad (1)$$

where, $\bar{\mathbf{X}}_i \in \mathbb{R}^{k_1k_2k_3\times(r-k_1+1)(s-k_2+1)}$ $(i \in [1, N])$is the patch mean removed version of $\mathbf{X}_i$. Assuming that the number of filters in the first stage is L_1, we employ PCA to learn the filter banks in this stage. The solution is known as the L_1 principal eigenvectors of $\mathbf{XX}^T$corresponding to larger eigenvalues. The learned filters are therefore expressed as

$$W_l^1 = \mathrm{mat}_{k_1,k_2}(q_l(\mathbf{XX}^T)) \in \mathbb{R}^{k_1\times k_2}, l = 1, 2, ..., L_1, \quad (2)$$

where, $\mathrm{mat}_{k_1,k_2}(v)$is a function that maps eigenvector to a matrix $W \in \mathbb{R}^{k_1\times k_2}$. $q_l(\mathbf{XX}^T) \in \mathbb{R}^{1\times k_1k_2}$denotes the L-th principal eigenvectors of $\mathbf{XX}^T$, which captures the main variation of all of the mean-removed patches in training images.

2.1.2. The second convolution stage

The second convolution stage almost repeat the same process in the first stage, let the output of L-th filter in the first stage be

$$I_i^l = I_i * W_l^1, I_i^l \in \mathbb{R}^{r\times s}, \ i \in [1, N], \quad (3)$$

where, $*$ denotes the convolution, and the boundary of I_i is zero-padded before convolving with W_l^1 to make I_i^lhave the same size as I_i. As same as the first stage, we collect all of the overlapping patches of I_i^l, subtract the patch mean from each patch and obtain

$$\mathbf{Y}^l=\left[\bar{\mathbf{Y}}_1^l,\bar{\mathbf{Y}}_2^l,\ldots,\bar{\mathbf{Y}}_N^l\right] \in \mathbb{R}^{k_1k_2\times N(r-k_1+1)(s-k_2+1)}, \quad (4)$$

concatenating $\mathbf{Y}^l$ for all the filter outputs as

$$\mathbf{Y}=\left[\mathbf{Y}^1,\mathbf{Y}^2,\ldots,\mathbf{Y}^{L_1}\right] \in \mathbb{R}^{k_1k_2\times L_1N(r-k_1+1)(s-k_2+1)}. \quad (5)$$

Please cite this article as: X. Bi, S. Li and B. Xiao et al., Computer aided Alzheimer's disease diagnosis by an unsupervised deep learning technology, Neurocomputing, https://doi.org/10.1016/j.neucom.2018.11.111

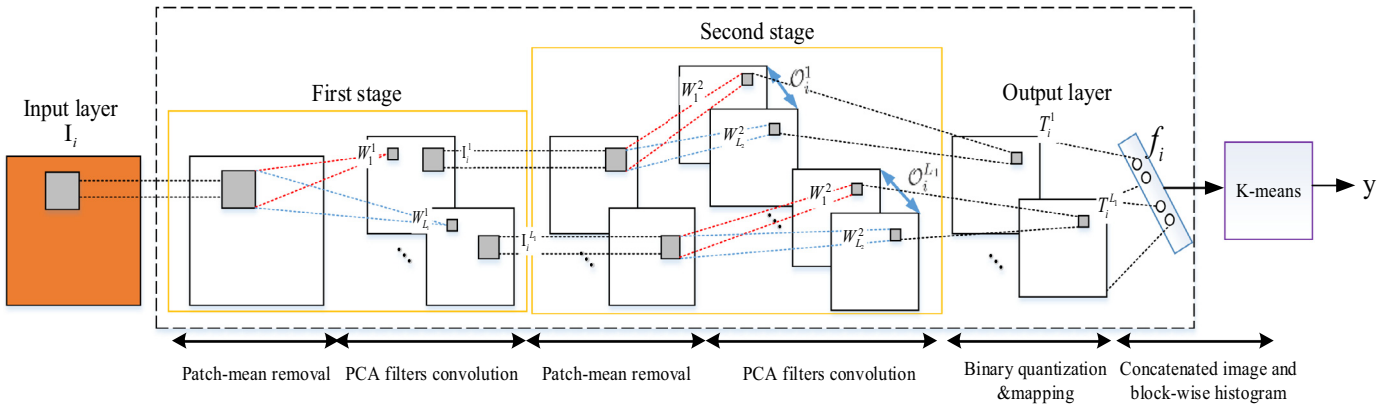

Fig. 1. Flow chart of the proposed PCANet+*k*-means clustering with one view of MRI image.

The filter banks $W_l^2$of the second stage are then learned by PCA algorithm as

$$W_l^2 = \mathrm{mat}_{k_1\times k_2}(q_l(\mathbf{YY}^T)) \in \mathbb{R}^{k_1\times k_2}, l = 1, 2, \ldots, L_2. \quad (6)$$

where, L_2 is the number of filters in the second convolution stage. Hereafter, the L_1 learned filters W_l^1 and L_2 learned filters $W_l^2$are utilized as the convolution filter banks in the first and second stages, respectively.

2.1.3. The output stage

This stage includes two steps: Hashing and histogram generating. Firstly, for each input matrix I_i^l of stage 2, we get

$$T_i^l = \sum_{l=1}^{L_2} 2^{l-1} H(I_i^l * W_l^2), \quad (7)$$

where, $H(\cdot)$ is a Heaviside step function, whose value is one for positive and zero for otherwise. Eq. (7) converts the L_2 outputs of the second stage back into a single integer valued matrix whose element values are in the range $[0,\ 2^{L_2}-1]$. Secondly, for each of the L_1 matrix $T_i^l,\ l \in [1,\ L_1]$, we partition it into B blocks, and compute the histogram of integer values in each block with 2^{L_2} bins. This is followed by concatenating all B histograms into a vector (denoted as $Bhist(T_i^l)$). At last, the feature vector f_i is estimated to a set of block-wise histograms for image representation:

$$f_i = \left[Bhist(T_i^1), \ldots, Bhist(T_i^{L_1})\right]^T \in \mathbb{R}^{1\times(2^{L_2})L_1 B}. \quad (8)$$

Moreover, in the histogram generating step, the local blocks of PCANet can be either overlapping or non-overlapping. In the proposed method, for reducing the length of feature vector, we use non-overlapping blocks.

The feature vector of input images can be extracted by the above three stages in PCANet. Those stages don't involve any hardly training processes and have many tricks in parameter setting. The hype-parameters in PCANet only include the filter size, the number of filters in each stage, and the block size for histograms in the output layer. Through the grid search with either cross-validation or a validation set, we can get the optimal filter size and the block size for local histograms. Moreover, the number of filters in each stage, and some fine-tuning on the number of filters are set according to marginal performance improvements. Once these parameters are fixed, the training procedure of the PCANet will become very simple and efficient, since the filter learning in the PCANet does not involve regularized parameters of requiring numerical optimization solvers.

2.2. K-means clustering algorithm

Clustering is a method to divide a set of data into a specific number of groups. One of the popular clustering methods is *k*-means clustering. The *k*-means clustering divides a collection of data into *k* number of disjoint cluster [28], and it consists of two separate phases: the first phase is mainly to estimate *k* centroid of each cluster, the second phase is to take each point belonging to a given data set and assign it to the nearest centroid. There are different methods to define the distance of nearest centroid. One of the commonly used methods is Euclidean distance. Once the grouping is done it recalculate the new centroid of each cluster. Based on the new centroid, a new Euclidean distance is calculated between each centroid and each data point, and then assigns the points in the cluster which have minimum Euclidean distance. Each cluster in the partition is defined by its member objects and centroid. When the sum of distances from all the objects in that cluster is minimized, the centroid and the cluster label for each cluster are determined over all clusters.

3. The proposed method

3.1. PCANet+k-means clustering with one view of MRI image

We propose the unsupervised method by using PCANet and *k*-means for computer aided AD prediction. The proposed method firstly utilizes one view of MRI image as the input data for predicting MRI image. The sagittal slice centered at the center of hippocampus in MRI image is fed into the PCANet. The PCANet can serve as a simple but surprisingly competitive baseline for empirically justifying advanced designs of multistage features or networks and can also be act as feature learner. As shown in Fig. 1, the procedure of learning feature consists four stages: the first convolutional stage, the second convolutional stage, the hashing (nonlinear) and histogram estimation (pooling) stages. Through these stages, the learned features from PCANet can be taken as input of the followed *k*-means clustering for prediction. The *k*-means clustering is adopted in the proposed method because of its simplicity and efficiency, and it is also an unsupervised classification method. Supposing a features matrix with size of $x \times y$, x represents the feature vector of each data point learned from PCANet, and y represents the number of data points (or subjects). Let p_y represents the feature vector, and c_k represents the cluster centroid, the main steps of *k*-means for AD prediction based on the features learned by PCANet are as follows:

(1) Initialize number of cluster *k* and the cluster centers (defined randomly).

Please cite this article as: X. Bi, S. Li and B. Xiao et al., Computer aided Alzheimer's disease diagnosis by an unsupervised deep learning technology, Neurocomputing, https://doi.org/10.1016/j.neucom.2018.11.111

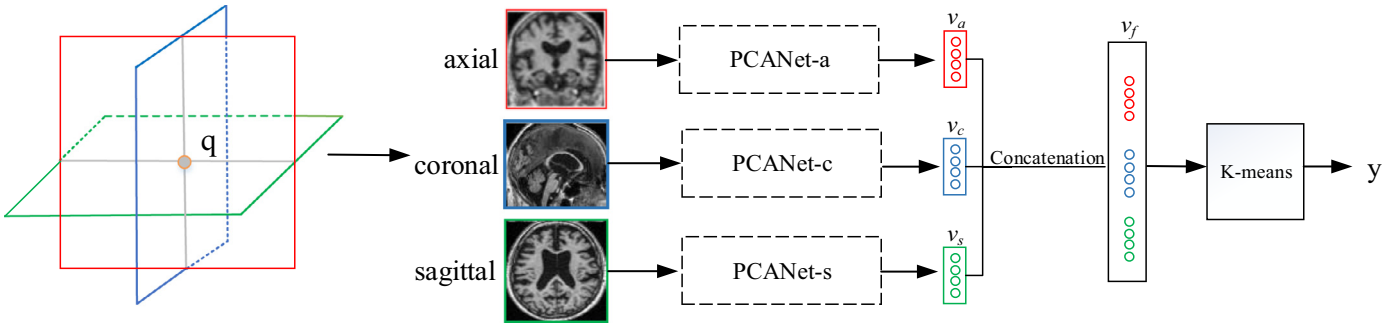

Fig. 2. Flow chart of proposed PCANet+*k*-means clustering with TOP data.

(2) For each data point, calculate the Euclidean distance *d*between the feature vector of current point and that of centroid.
(3) Assign the point to the nearest centroid based on distance *d*.
(4) After all data points have been assigned, recalculate the new centroid of each cluster and renew the centroid.
(5) Repeat steps 2–4 until the sum of distances from all the points in that cluster is minimized.

The *k*-means algorithm partitions a set of subjects into *k* clusters, and the output of *k*-means is the cluster label for each subject. Comparing the cluster label with the real label corresponds to the MRI subjects, we can obtain the final prediction accuracy.

3.2. PCANet+k-means clustering with TOP views of MRI image

Although one view of an MRI image can obtain acceptable results in AD prediction, when the number of subjects increased, the input data with one slice cannot catch enough information to discriminate AD. On the contrary, the processes of feature extraction are time consuming and some extra information are involved if all of the slices are used. Therefore, in the proposed method, we can use three views of MRI image in the form of three orthogonal planes (TOP) for feature extraction. As shown in Fig. 2, three slices is corresponded to axial, coronal and sagittal (indicated as {*a, c, s*}) view of an MRI image, the center of hippocampus are fed to the PCANet for features extraction respectively. We obtain the three feature vectors $\{v_a, v_c, v_s\}$, and then concatenate the three features as the final features v_f of the subject. Through above stages, the learned features v_f from PCANet can be taken as input of the followed *k*-means clustering for prediction. Similar with the clustering processes introduced in Section 3.1, the *k*-means clustering algorithm is employed for dividing a set of feature vectors into *k* clusters. Then we can obtain the prediction label for each feature vector and compare it with the real label of the feature vector to get the final prediction accuracy.

4. Experiments

4.1. Experiment dataset

The experiment data used in the preparation of this paper is obtained from Alzheimer's disease Neuroimaging Initiative (ADNI) database (http://adni.loni.usc.edu/). The ADNI was launched in 2003 by the National Institute on Aging (NIA), the National Institute of Biomedical Imaging and Bioengineering (NIBIB), and the Food and Drug Administration (FDA). The primary goal of ADNI is to test whether serial MRI, PET, other biological markers, and clinical and neuropsychological assessment can be combined to measure the progression of MCI and early AD. Determination of sensitive and specific markers of very early AD progression is intended to aid researchers and clinicians to develop new treatments and monitor their effectiveness, as well as lessen the time and cost of clinical trials. In our experiments, the MRI image collection "ADNI1: Screening 1.5T" with 1075 subjects who have a screening scan is used for AD prediction. Those subjects were grouped as three classes: (1) AD (Alzheimer's disease), if screen diagnosis was Alzheimer's disease (243 subjects); (2) NC (Normal cognitive), if screen diagnosis was normal (307 subjects); (3) MCI (Mild cognitive impairment), if screen diagnosis was mild cognitive impairment (525 subjects).

4.2. Image preprocessing

The MRI images are normalized into an International Consortium for Brain Mapping template by Statistical Parametric Mapping (SPM12)[1] toolbox. Our configuration also includes a positron density template with no weighting image, and a 7th-order B-spline for interpolation. The remaining parameters were set to their default. The dimension of normalized image is $79 \times 95 \times 79$. The TOP views of MRI image are obtained by the MRIcron [29] software with changing the position of the cross at the center of the hippocampus in each image. Fig. 3 shows an example of the TOP slices obtained from a normalized MRI image.

4.3. Experiment results

In our experiments, we utilize the preprocessed MRI data with 1075 subjects as input data, and evaluated the performance of the proposed method from the prediction accuracy for each AD/NC, AD/MCI, MCI/NC, and AD/MCI/NC group. In the proposed method, MRI data are fed to the PCANet for feature extraction. The parameters of PCANet are set as followed. The filter size of the network is $k_1 = k_2 = 5$, and their non-overlapping blocks are of size 8×8, the number of filters $L_1 = L_2 = 8$. When these parameters are fixed, we can learn the features of AD through the first convolution stage, the second convolution stage, and the output stage.

The unsupervised predictor in our method are all selected as *k*-means clustering. We evaluate the prediction performance of the proposed method from aspect of prediction accuracy analysis for each AD/NC, AD/MCI and MCI/NC group. The number of cluster is set to $k = 2$, since there are only two categories in each group. Furthermore, although *k*-means has the great advantage of being easy to implement, the quality of the final clustering results depends on the arbitrary selection of initial centroid. If the initial centroid is randomly chosen, it will get different result for different initial centers. Therefore, in each experiment, the classification task

[1] The SPM 12 toolbox can be downloaded from http://www.fil.ion.ucl.ac.uk/spm/.

Please cite this article as: X. Bi, S. Li and B. Xiao et al., Computer aided Alzheimer's disease diagnosis by an unsupervised deep learning technology, Neurocomputing, https://doi.org/10.1016/j.neucom.2018.11.111

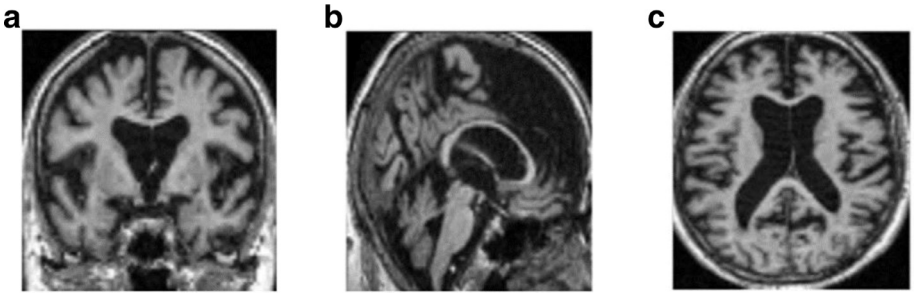

Fig. 3. Three TOP slices of a MRI image of an AD patient, from left to right: (a) in axial view, (b) coronal view and (c) sagittal view.

Table 1
Classification performance of the proposed method with different views of MRI image from the aspects of prediction accuracy.

Methods	Subject sizes	Classification accuracy	
PCANet+k-means clustering with sagittal view of MRI image	243 AD	AD vs. MCI	95.52%
		AD vs. NC	76.32%
		MCI vs. NC	90.63%
		AD vs. MCI vs. NC	89.38%
	307 NC	Average	87.96%
PCANet+k-means clustering with TOP views of MRI image	525 MCI	AD vs. MCI	97.01%
		AD vs. NC	89.15%
		MCI vs. NC	92.6%
		AD vs. MCI vs. NC	91.25%
		Average	92.5%

Table 2
Review of some other methods for AD prediction. The subject size and the classification accuracy of these methods are also provided.

Methods	Subject sizes	Classification accuracy
[17]	198 AD,409 MCI (pMCI and sMCI), 231 NC	AD vs. NC 87.9% pMCI vs. NC 83.2% pMCI vs. sMCI 70.4%
[30]	202 AD, 410 MCI, 236 NC	75% of data in training set: AD vs. NC 78.4% MCI vs. NC 71.2% 90% of data in training set: AD vs. NC 85.7% MCI vs. NC 79.2%
[31]	56 AD, 60 MCI, 60 NC	AD vs. NC 89% MCI vs. NC 72%
[8]	198 AD, 238 sMCI, 167 pMCI 234 NC	AD vs. NC 88.8% pMCI vs. sMCI 69.6%
[32]	65 AD, 67 cMCI, 102 ncMCI, 77 HC	AD vs. NC 87.76% MCI vs. NC 76.92%
[21]	211 AD, 91 NC	AD vs. NC 98.84% (with spatially smoothing) AD vs. NC 84.50% (without spatially smoothing) AD vs. MCI *NaN* MCI vs. NC *NaN*
[23]	70 AD, 70 MCI, 70 NC	AD vs. NC 97.6% AD vs. MCI 95% MCI vs. NC 90.8%

is repeated ten times, and the average of ten prediction results is taken as the final prediction accuracy. Table 1 shows the final prediction accuracy of the proposed method for each AD/NC, AD/MCI and MCI/NC group. The clustering results based on MRI image with one sagittal view are described in Fig. 4, and the clustering results based on MRI image with TOP views of MRI image are shown in Fig. 5,

In recent years, several methods have been proposed to classify the subjects based on MRI image for AD prediction. Since these methods used different datasets and preprocessing methods, a direct comparison of these methods is difficult to achieve. A selection of related methods along with the subject size and the reported performance is given in Table 2. The method proposed in [17] combined penalized regression and data resampling for feature extraction, and a SVMs classifier with Gaussian kernels was followed for AD prediction. In [30], the independent component analysis (ICA) was used as a feature extractor and coupled with a SVM classifier for AD prediction. The method proposed in [31] used SVM classifier with the bagging method for AD vs. NC and a logistic regression model with a boosting algorithm for MCI vs. NC. In [8], the authors achieved the AD prediction through extracting local intensity patches and applying a graph-based multiple instance learning technique. Recently, deep learning methods have also been investigated for AD prediction based on MRI images. The authors in [32] utilized a deep fully-connected network pre-trained with stacked autoencoders which is then fine-tuned for AD prediction. The method [21] outlined deep learning-based pipelines to distinguish Alzheimer's MRI and fMRI from normal healthy control data for a given age group, and it well distinguished Alzheimer's patients from healthy normal brains. The authors in [23] proposed a method for AD prediction with a deep 3D convolutional neural network, which is pre-trained to capture anatomical shape variations in structural brain MRI image.

5. Discussion

In this paper, we have presented a fully unsupervised method with different views of MRI image to achieve automatic prediction of patients with Alzheimer's disease from MRI images. In the first stage, we present the PCANet which the filter banks are prefixed by the conventional unsupervised machine learning method to learn the features of one view of MRI image for each subject. This is followed by an unsupervised classification method, which is based on k-means clustering to achieve the final prediction. This method obtains prediction accuracy 95.52% for AD vs. MCI, 76.32% for AD vs. NC, 90.63% for MCI vs. NC, 89.38% for AD vs. MCI vs. NC on all the 1075 subjects in ADNI database. The average prediction accuracy of the first method is 87.96%, which demonstrates the effectiveness of the proposed method. Moreover, we also verify the prediction performance, which utilize the TOP slices of MRI image for AD prediction. We employ PCANet to extract three feature vectors corresponding to the TOP slices of each subject respectively, and concatenate these three feature vectors as the final feature vector of the subject. Then a k-means clustering is followed for AD prediction. This proposed method achieves prediction accuracy to 97.01% for AD vs. MCI, 89.15% for AD vs. NC, 92.6% for MCI vs. NC, 91.25% for AD vs. MCI vs. NC on all the 1075 subjects in ADNI database. The average accuracy of the second method is up to 92.5%, which

Please cite this article as: X. Bi, S. Li and B. Xiao et al., Computer aided Alzheimer's disease diagnosis by an unsupervised deep learning technology, Neurocomputing, https://doi.org/10.1016/j.neucom.2018.11.111

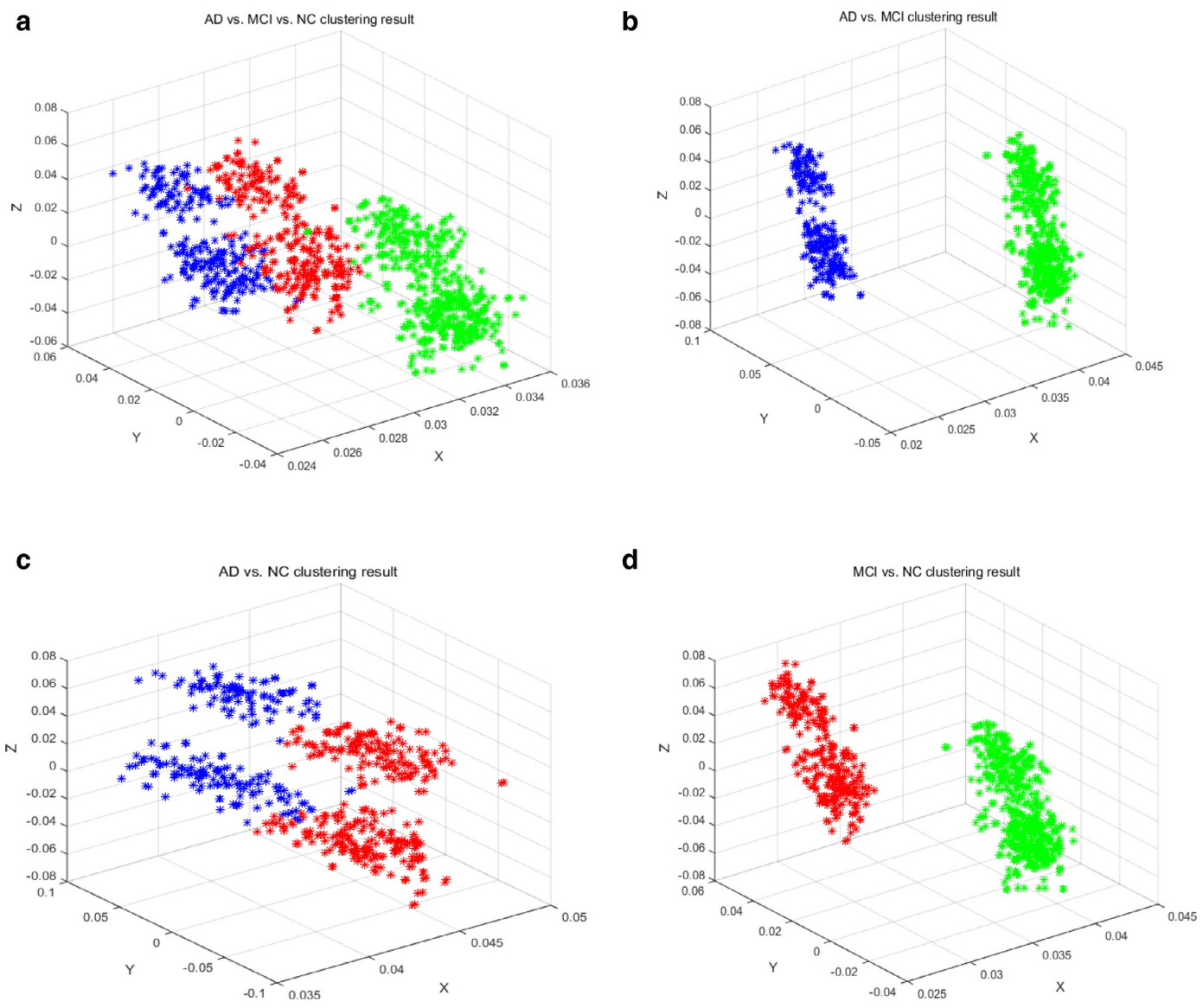

Fig. 4. Clustering result for (a) AD vs. MCI vs. NC, (b) AD vs. MCI, (c) AD vs. NC and (d) MCI vs. NC based on MRI image with one slice. Blue points indicate AD subjects, green points indicate MCI subjects and red points indicate NC subjects. Axis *X*, *Y* and *Z* represents the three features correspond to three largest eigen values among the feature vectors of all subjects.

is the highest performance among these methods. From the visualization of clustering result shown in Fig. 4, it can be found that the clustering result is obvious, and the distance between clusters is distinguished. At the same time, Fig. 4(c) is also can be used for explaining why our proposed methods achieve lower prediction accuracy on AD vs. NC group than other groups. The tendency of *k*-means to produce equal-sized clusters leads to bad results since the distributions of AD and NC is ellipse shaped.

From the performance of the proposed method, it can be found that, although one slice of MRI image as the input data of the proposed method can achieve acceptable results in AD prediction, the TOP slices of MRI image as the input data achieves obviously higher classification accuracy (PCANet with TOP slices achiever 4.54% higher than PCANet with one slice in average accuracy). This can be explained by two reasons. Firstly, input data with on slice catch enough discriminatory information to prediction the AD. Secondly, the TOP slices centered at the center of hippocampus catches more information of anatomical structures such as gray matter, white matter, cerebrospinal fluid (CSF) and hippocampus that have been proven the effectiveness in AD prediction [33].

Compared with the state-of-the-art methods in AD prediction, the proposed method achieves promising performance, i.e., up to 92.5% average prediction accuracy on the image collection "ADNI1: Screening 1.5T" with 1075 subjects. While, as shown in Table 2, some existing methods obtained slightly lower prediction accuracy on limited number of subjects or with data selected on a specific image collection. Furthermore, it can be found from Table 2 that, recent proposed methods [21] and [23] perform better than our proposed method. This can be explained as follows: (1). In [21], the data with two modalities combined (rs-MRI and MRI) were used for AD prediction, and only 302 subjects with MRI modality

Please cite this article as: X. Bi, S. Li and B. Xiao et al., Computer aided Alzheimer's disease diagnosis by an unsupervised deep learning technology, Neurocomputing, https://doi.org/10.1016/j.neucom.2018.11.111

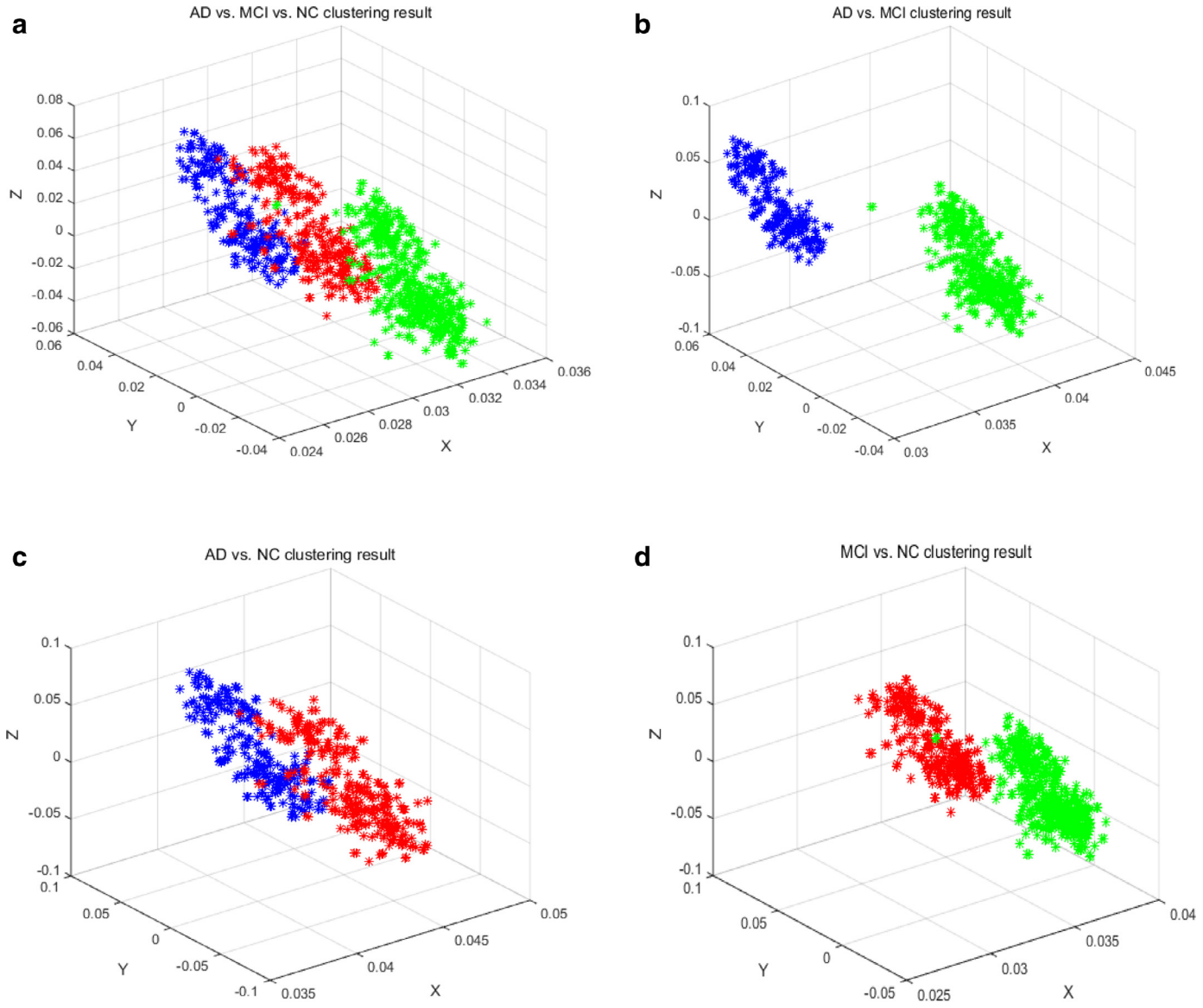

Fig. 5. Clustering result for (a) AD vs. MCI vs. NC, (b) AD vs. MCI, (c) AD vs. NC and (d) MCI vs. NC based on MRI image with TOP slices. Blue points indicate AD subjects, green points indicate MCI subjects and red points indicate NC subjects. Axis *X*, *Y* and *Z* represents the three features correspond to three largest eigen values among the feature vectors of all subjects.

in ADNI database are selected for validation. (2). Method [21] utilized a specified prepossessing step that spatially smoothed each subject by sigma= 3 mm, and the prediction accuracy decreased to 84.50% if this smooth step is canceled. (3). Method [23] used the CADDe-mentia database which only includes MCI and NC subjects (without AD subjects) to pre-train a 3-D convolutional autoencoder. This is followed by fine-tuned fully connected upper layers of the 3D-CNN for each task-specific AD classification, and 94.47% average prediction accuracy was achieved. Similar with method [21], in method [23], only 210 subjects (70 subjects for each category) in ADNI database are selected for validation. On the contrary, in our proposed method, only one modality is used and all of the subjects (1075 subjects, without any data selection or exclusion) with MRI modality in ADNI database are chosen for validation. The average prediction accuracy of our proposed method is only 1.9% lower than method [23] while the scale of database our proposed method implemented on is much large than that of [23].

6. Conclusions

We regarded our work as an idea evidence that employing the fully unsupervised method to achieve the automatic prediction of patients with Alzheimer's disease only from MRI image. We firstly used an unsupervised CNN model which is based on PCANet to learn the features from MRI images, and then used an unsupervised classification method which is based *k*-means clustering to achieve the classification task. Experimental results show that, the proposed method achieves 92.5% average prediction accuracy (97.01% for AD vs. MCI, 89.15% for AD vs. NC, 92.6% for MCI vs. NC, and 91.25% for AD vs. MCI vs. NC) for AD prediction on all the 1075 subjects of ADNI without only data selection or exclusion. We have also compared the performance of proposed approach with state of the art methods in AD prediction. The performance of the proposed methods is promising, and it proves that the proposed methods can be implemented as parts of a CAD systems for efficient AD diagnosis.

Please cite this article as: X. Bi, S. Li and B. Xiao et al., Computer aided Alzheimer's disease diagnosis by an unsupervised deep learning technology, Neurocomputing, https://doi.org/10.1016/j.neucom.2018.11.111

The proposed methods also have some limitations and potentials which will be investigated in our future work, e.g., (1) fine tuning the *k*-means method, or employing other clustering algorithms such as *k*-means++, Gaussian mixture models, etc., to improve the prediction accuracy for AD diagnosis; (2) combining the 3D-PCANet method with *k*-means that full 3D input data is used to achieve the AD prediction; (3) further verifying the proposed methods with even larger scale database.

Conflict of interest

None.

Acknowledgments

Dataset used in this paper is obtained from the Alzheimer's disease Neuroimaging Initiative (ADNI) database (http://adni.loni.usc.edu). As such, the investigators within the ADNI contributed to the design and implementation of ADNI and/or provided data but did not participate in the analysis or writing of this report. A complete listing of ADNI investigators can be found at https://adni.loni.usc.edu/wp-content/uploads/how_to_apply/ADNI_Acknowledgement_List.pdf. The authors would like to thank the anonymous referees for their valuable comments and suggestions.

This work was partly supported by the National Science & Technology Major Project (2016YFC1000307-3), the National Natural Science Foundation of China (61572092 and 61806032), the Chongqing Research Program of Application Foundation & Advanced Technology (cstc2018jcyjAX0117) and the Scientific & Technological Key Research Program of Chongqing Municipal Education Commission (KJZD-K201800601).

References

[1] A. Payan and G. Montana, Predicting Alzheimer's disease: a neuroimaging study with 3D convolutional neural networks. arXiv preprint arXiv:1502.02506, 2015.
[2] J. Han, D. Zhang, G. Cheng, N. Liu, D. Xu, Advanced deep-learning techniques for salient and category-specific object detection: a survey, IEEE Signal Process. Mag. 35 (1) (2018) 84–100.
[3] A. Association, 2014 alzheimer's disease facts and figures, Alzheimers Dement. 10 (2014) e47.
[4] E.E. Bron, M. Smits, V.D.F. WM, H. Vrenken, F. Barkhof, P. Scheltens, Standardized evaluation of algorithms for computer-aided diagnosis of dementia based on structural MRI: the CADDementia challenge, Neuroimage 111 (2015) 562–579.
[5] J. Han, R. Quan, D. Zhang, F. Nie, Robust object co-segmentation using background prior, IEEE Trans. Image Process. 27 (4) (2018) 1639–1651.
[6] M. Grundman, R.C. Petersen, S.H. Ferris, R.G. Thomas, P.S. Aisen, D.A. Bennett, Mild cognitive impairment can be distinguished from Alzheimer disease and normal aging for clinical trials, Arch. Neurol. 61 (2004) 59.
[7] K.R. Gray, P. Aljabar, R.A. Heckemann, A. Hammers, D. Rueckert, Random forest-based similarity measures for multi-modal classification of Alzheimer's disease, Neuroimage 65 (2012) 167–175.
[8] T. Tong, R. Wolz, Q. Gao, J.V. Hajnal, D. Rueckert, Multiple instance learning for classification of dementia in brain MRI, Med. Image Anal. 18 (2014) 808–818.
[9] J. Han, G. Cheng, Z. Li, D. Zhang, A unified metric learning-based framework for co-saliency detection, IEEE Trans. Circuits Syst. Video Technol. doi:10.1109/TCSVT.2017.2706264.
[10] C.Y. Wee, P.T. Yap, D. Zhang, K. Denny, J.N. Browndyke, G.G. Potter, Identification of MCI individuals using structural and functional connectivity networks, Neuroimage 59 (2012) 2045.
[11] B. Jie, C.Y. Wee, D. Shen, D. Zhang, Hyper-connectivity of functional networks for brain disease diagnosis, Med. Image Anal. 32 (2016) 84.
[12] C.Y. Wee, P.T. Yap, D. Zhang, L. Wang, D. Shen, Group-constrained sparse fMRI connectivity modeling for mild cognitive impairment identification, Brain Struct. Funct. 219 (2014) 641.
[13] R. Wolz, V. Julkunen, J. Koikkalainen, E. Niskanen, D.P. Zhang, D. Rueckert, Multi-method analysis of MRI images in early diagnostics of Alzheimer's disease, PLoS One 6 (2011) e25446.
[14] C. Chu, A.L. Hsu, K.H. Chou, P. Bandettini, C. Lin, Does feature selection improve classification accuracy? Impact of sample size and feature selection on classification using anatomical magnetic resonance images, Neuroimage 60 (2012) 59–70.
[15] G. Cheng, P. Zhou, J. Han, Duplex metric learning for image set classification, IEEE Trans. Image Process. 27 (1) (2018) 281–292.
[16] M. Liu, D. Zhang, D. Shen, Ensemble Sparse classification of Alzheimer's disease, Neuroimage 60 (2012) 1106.
[17] E. Janoušová, M. Vounou, R. Wolz, K.R. Gray, D. Rueckert, G. Montana, Biomarker discovery for sparse classification of brain images in Alzheimer's disease, Annals of the BMVA 2012 (2) (2012) 1–11.
[18] E. Hosseiniasl, M. Ghazal, A. Mahmoud, A. Aslantas, A.M. Shalaby, M.F. Casanova, Alzheimer's disease diagnostics by a deeply supervised adaptable 3D convolutional network, Front. Biosci. 23 (2016) 584–596.
[19] G. Cheng, C. Yang, X. Yao, L. Guo, J. Han, When deep learning meets metric learning: remote sensing image scene classification via learning discriminative CNNs, IEEE Trans. Geosci. Remote Sens. 56 (5) (2018) 2811–2821.
[20] H. Choi, H. Jin K, Predicting cognitive decline with deep learning of brain metabolism and amyloid imaging, Behav. Brain Res. 344 (2017) 103–109.
[21] B. Xiao, K. Wang, X. Bi, W. Li, J. Han, 2D-LBP: An enhanced local binary feature for texture image classification, IEEE Trans. Circuits Syst. Video Technol. doi:10.1109/TCSVT.2018.2869841.
[22] S. Sarraf, G. Tofighi, Classification of alzheimer's disease using fmri data and deep learning convolutional neural networks. arXiv preprint arXiv:1603.08631, 2016.
[23] E. Hosseini-Asl, R. Keynton, A. El-Baz, Alzheimer's disease diagnostics by adaptation of 3D convolutional network, in: Proceedings of IEEE International Conference on Image Processing, ICIP, 2016.
[24] M. Liu, et al., Multi-modality cascaded convolutional neural networks for Alzheimer's disease diagnosis, Neuroinformatics 16 (2018) 1–14.
[25] A. Farooq, et al., A deep CNN based multi-class classification of Alzheimer's disease using MRI, in: Proceedings of IEEE International Conference on Imaging Systems and Techniques, 2018, pp. 1–6.
[26] B. Xiao, L. Li, Y. Li, W. Li, G. Wang, Image analysis by fractional-order orthogonal moments, Inf. Sci. 382 (2017) 135–149.
[27] T.H. Chan, K. Jia, S. Gao, J. Lu, Z. Zeng, Y. Ma, PCANet: a simple deep learning baseline for image classification? IEEE Trans. Image Process. 24 (2015) 5017–5032.
[28] N. Dhanachandra, K. Manglem, Y.J. Chanu, Image Segmentation using K-means clustering algorithm and subtractive clustering algorithm, Procedia Comput. Sci. 54 (2015) 764–771.
[29] MRIcron: http://www.nitrc.org/projects/mricron, 2015.
[30] W. Yang, R.L. Lui, J.H. Gao, T.F. Chan, S.T. Yau, R.A. Sperling, X. Huang, Independent component analysis-based classification of Alzheimer's disease MRI data, J. Alzheimer's Dis. 24 (2011) 775–783.
[31] N. Batmanghelich, B. Taskar, C. Davatzikos, A general and unifying framework for feature construction, in image-based pattern classification, in: Proceedings of International Conference on Information Processing in Medical Imaging, 2009, pp. 423–424.
[32] S. Liu, S. Liu, W. Cai, S. Pujol, R. Kikinis, D. Feng, Early diagnosis of Alzheimer'sdisease with deep learning, in: Proceedings of IEEE International Symposium on Biomedical Imaging, IEEE, 2014, pp. 1015–1018.
[33] R. Cuingnet, E. Gerardin, J. Tessieras, G. Auzias, S. Lehéricy, M.O. Habert, Automatic classification of patients with Alzheimer's disease from structural MRI: a comparison of ten methods using the ADNI database, Neuroimage 56 (2011) 766–781.

Xiuli Bi received his B.Sc. and M.Sc. degrees from Shannxi Normal University, China, in 1995 and 1998, respectively, and Ph.D. degree in Computer Science from the University of Macau in 2017. She is currently a lecture at the College of Computer Science and Technology, Chongqing University of Posts and Telecommunications, China. Her research interests include image processing; multimedia security and image forensics.

Shutong Li was born in 1992. He is currently pursuing the M.S. degree at Chongqing University of Post and Telecommunications. His research interests include medical image processing and pattern recognition.

Bin Xiao was born in 1982. He received his B.S. and M.S. degrees in Electrical Engineering from Shaanxi Normal University, Xian, China in 2004 and 2007, received his Ph.D. degree in computer science from Xidian University, XiAn, China. He is now a professor at Chongqing University of Posts and Telecommunications, Chongqing, China. His research interests include image processing and pattern recognition.

Yu Li received the B.E. and M.E. degrees in electrical engineering from Xidian University, China, in 2002 and 2006, and a Ph.D. in Biomedical Engineering from The University of Queensland, Australia, in 2011. He is currently working as a postdoctoral research fellow in the School of Information Technology and Electrical Engineering at the University of Queensland. He works on the field of biomedical engineering and focuses on Magnetic Resonance Imagining (MRI). His current research interests include MR engineering (electromagnetic analysis in MRI, key hardware design); fast MRI imaging and image processing; computational electromagnetics, etc.

Guoyin Wang was born in 1970. He received the bachelor's degree in computer software, the master's degree in computer software, and the Ph.D. degree in computer organization and architecture from Xi'an Jiaotong University, Xi'an, China, in 1992, 1994, and 1996, respectively. He is the author of over 200 reviewed research publications. His books and papers have been cited over 6000 times. His research interests include data mining, machine learning and pattern recognition.

Xu Ma was born in 1963. He received his master degree of genetics from West China University of Medical Science, Chengdu, China. He is the professor of Peking Union Medical College. He had published over 280 papers. His research interests include genetics, epidemiology and statistics.

Please cite this article as: X. Bi, S. Li and B. Xiao et al., Computer aided Alzheimer's disease diagnosis by an unsupervised deep learning technology, Neurocomputing, https://doi.org/10.1016/j.neucom.2018.11.111